FERMILAB-PUB-77-165-E
UR-623
COO-3065-174

Coherent Dissociation of Neutrons on Nuclei at 100-300 GeV/c*

W. Mollet#, J. Biel†, T. Ferbel, P. Slattery and D. Underwood‡

University of Rochester

Rochester, N.Y. 14627

CONTRACT NUMBER EY-76-c-02-3065.000

and

B. Gobbi, L. Kenah**, J. Rosen and R. Ruchti##

Northwestern University

Evanston, Ill. 60201

and

E. Bleser

Fermilab

Batavia, Ill. 60510

and

D. Freytag

SLAC

Stanford, CA. 94305

Abstract

We have observed the coherent dissociation of neutrons into $p\pi^-$ systems at incident momenta up to 300 GeV/c. We present the dissociation cross sections for a viariety of nuclear targets for $p\pi^-$ masses below 1.85 GeV. Using a model incorporating both electromagnetic and hadronic production, we have extracted the total cross sections for scattering of unstable $p\pi^-$ systems on nucleons.

*Research supported by the U.S. Energy Research and Development Administration. University of Rochester Report UR-623, Northwestern University Report NW-EXP-7.

#Deceased
†Presently at Fermilab, Batavia, Ill. 60510.
‡Presently at ANL, Argonne, Ill. 60439.
**Presently at DEC, Maynard, Mass. 01754
##Presently at Notre Dame, Notre Dame, Ind. 46556

Submitted to Phys. Rev. Letters.
September 1977

We have measured the dissociation of neutrons into $p\pi^-$ systems on the nuclear targets Be, C, Al, Ti, Cu, Ag, Ta and Pb, for neutron momenta in the range 100-300 GeV/c. The experiment was performed in the M3 neutral beam at Fermilab. The apparatus was described in a previous Letter[1] which concerned our study of dissociation using a hydrogen target. The measurements using nuclear targets differ in that no total absorption calorimeter was present at the downstream end of the apparatus, and the use of a solid target precluded any measurement of the recoiling nucleus. In this Letter we present the measured dissociation cross sections, and the total cross sections for the scattering of the produced states on nucleons; the latter are determined indirectly with the aid of an eikonal model. A detailed comparison of the $p\pi^-$ decay angular distributions for the nuclear and hydrogen[2] data will be presented elsewhere. Similar measurements of neutron dissociation at lower energies have been reported previously in the literature[3]. Although, for brevity, in this paper we shall often refer to $p\pi^-$ systems as N^*s, this should not imply that these systems are necessarily resonant or of unique isotopic spin.

We restrict our discussion to N*'s with invariant masses (m) in the range 1.165 to 1.85 GeV. Below 1.140 GeV, the extremely small opening angle of the proton and pion degrades the mass resolution and causes reconstruction losses which are difficult to assess in an accurate manner. Above 1.165 GeV, the mass resolution is $\sim$15 MeV (standard deviation), the reconstruction efficiency is $\sim$97%, and the spectrometer acceptance is always larger than 50% and, typically, about 75% for N* masses less than 1.85 GeV. All cross sections presented here have been corrected for acceptance, as well as for losses due to δ-rays striking the veto counters around the target (5-11%), and for small

spark chamber inefficiencies (typically 5%). Target empty corrections ranged from 4% to 20%, depending on the mass range and the specific target considered. The absolute normalization of the data is estimated as good to ±10%, whereas relative normalization between elements is good to better than ±3%.

A final, potentially important, correction to the data is the background due to other coherent dissociation processes, such as $n+A \rightarrow p\pi^-\pi^0+A$, or $n+A \rightarrow n\pi^+\pi^-+A$, and that due to incoherent $p\pi^-$ production. From Monte Carlo simulations we estimate that for events with small four-momentum transfers, $t'=|t-t_{min}| < 0.03\ (\mathrm{GeV}/c)^2$, these backgrounds are approximately 15% for $m < 1.3$ GeV, and about 5% at the highest masses.

Coherent dissociation can proceed either through the strong nuclear force or through an electromagnetic interaction between the incident neutron and the nuclear Coulomb field. The atomic number dependence of the coherent diffractive production reaction, $n+A \rightarrow p\pi^-+A$, is strongly affected by the total cross section of the produced $p\pi^-$ system on nucleons. The nuclear diffractive cross section for a given mass range (Δm) and t' range ($\Delta t'$) is given in the optical model by:[4]

$$\sigma_{diff}(\Delta m,\Delta t') = \int_{\Delta m} dm \int_{\Delta t'} dt' \left| f_H(t')\cdot AF(\sigma_1,\alpha_1,\sigma_2,\alpha_2,c,a,t',m)\right|^2 \tag{1}$$

where $|f_H(t')|^2 \equiv C_o \exp(-bt')$ is the cross section on hydrogen.

The eikonal approximation for the nuclear form factor F which we use is discussed in detail in the paper by Kölbig and Margolis[4]. We have used $c = 1.12A^{1/3}$ fermis, and $a = .545$ fm for the parameters describing the nuclear half-density radius, and skin thickness, respectively. The total neutron-nucleon cross section (σ_1) and the ratios of the real to imaginary

parts of the forward elastic amplitudes for both the incoming and outgoing systems (α_1,α_2) have been fixed at 39mb and 0, respectively.[5] In comparing this model to experimental results, it is common to take C_0, b, and σ_2 as free parameters describing production on hydrogen. These parameters are somewhat coupled, and a reduction in the value of C_0 can often be accommodated, without a large increase in the χ^2 for a fit, by a corresponding reduction in σ_2. In our analysis, we have fixed the values of C_0 and b to be those directly measured in the hydrogen experiment.[1]

The extraction of σ_2 at these energies is somewhat complicated by the fact that the one-photon exchange contribution is in some cases considerably larger than the strong interaction cross section. In the absence of interference between the diffractive and electromagnetic processes[6], the additional contribution to coherent dissociation from Coulomb production, for a target of charge Z, will be

$$\sigma_{coul}(\Delta m,\Delta t) = \int_{\Delta m} dm \int_{\Delta t} dt \, \frac{Z^2\alpha}{\pi} \, \frac{\sigma_\gamma(m)}{(m^2-m_n^2)} \, \frac{t'}{t^2} \, |F_{em}|^2 \qquad (2)$$

where $\sigma_\gamma(m)$ is the cross section for the $\gamma + n \rightarrow \pi^- + p$, at the γ-n center of mass energy specified by m.[7] The detailed definition of the electromagnetic form factor F_{em} is given in references 8 and 9. Because Coulomb production occurs primarily at extremely large distances from the nucleus[10], this contribution to the coherent cross section is essentially independent of any reasonable variation of the parameters $\sigma_1,\sigma_2,\alpha_1,\alpha_2$,c and a.

Figure 1 serves to indicate the sensitivity of the data to various possible values of σ_2. Figure 1(a) displays the t'-dependence in Cu for neutron momenta between 200 GeV/c and 260 GeV/c, and for $1.35 < m < 1.45$ GeV; Fig. 1(b) provides, for the same mass and momentum band, the dependence of the cross section on A. The solid curves represent the sums of the model

calculations for σ_{diff} (as a function of σ_2) and σ_{coul}. The Coulomb contribution alone is shown as a dashed line. In all of our calculations we have included the effects of finite experimental resolution in t'.[11]

Figure 2 shows the mass spectra for two different regions of t': (a) $t' < .001$ $(GeV/c)^2$ where Coulomb production is most important, and (b) $0.005 < t' < .03$ $(GeV/c)^2$, which, particularly for the lower-z targets, includes most of the coherent signal. The data in Fig. 2 indicate substantial Coulomb production of $\Delta(1236)$, especially at small t', where the cross section is also approximately proportional to Z^2. The calculated contribution from Coulomb production in Pb is shown as a shaded band in Fig. 2(a). The width of the band indicates the uncertainty in the calculation due to the uncertainty in the measurement of $\sigma_\gamma(m)$. The calculation agrees with the Pb data up to a mass of $\sim$1.3 GeV, beyond which a contribution from diffractive production becomes apparent. The cross section for diffractive dissociation appears to peak at a mass of $\sim$1.35 GeV (see Fig. 2b).

The energy dependence of the production cross section for several mass intervals and targets is shown in Table I. The cross sections are essentially independent of momentum, except for elements with large Z, where some increase with momentum is expected due to the contribution from electromagnetic production in these elements.

Figure 2(c) displays the results of our extraction of σ_2. The large uncertainty in σ_2 for the lowest mass band is partly due to the fact that the hadronic component of the cross section which is sensitive to σ_2, is small compared to the electromagnetic part. Moreover, there is a fairly large uncertainty (±15%) in the Coulomb calculation for this mass interval due to discrepancies in the various photoproduction experiments.[7]

Nevertheless, it is clear that the extracted N*-nucleon total cross sections are considerably lower, particularly at large masses, than the neutron-nucleon cross section. This result is similar to that reported recently in an investigation of coherent production of $p\pi^+\pi^-$ systems at lower incident momenta.[12]

Finally, we wish to point out that the value of σ_2 may be a function of the spin state of the N*.[13] Because the M-3 neutron beam is unpolarized, we cannot extract the dependence of σ_2 on specific angular momentum states of the produced N* systems. Furthermore, it has been shown by Fäldt,[14], that neglecting possible nucleon helicity-flip contributions to coherent production (as was done in the model of ref. 4), can lead to an underestimate of the apparent value of the N*-nucleon total cross section, particularly at larger N* mass values. Calculations are presently in progress to gauge the sensitivity of σ_2 to such helicity-flip terms in coherent production.

We than Drs. P. Koehler, R. Lundy and J. Sanford for their support and encouragement.

References

1. J. Biel, et al., Phys. Rev. Lett. 36, 504 (1976).

2. J. Biel, et al., Phys. Rev. Lett. 36, 507 (1976); J. Biel, Ph.D. Thesis, University of Rochester, Report UR-614 (1977).

3. D. O'Brien et al., Nucl. Phys. B77, 1 (1974); W. Carithers et al., University of Rochester Report (submitted to London Conference-1974).

4. K. Kölbig and B. Margolis, Nucl. Phys. B6, 85 (1968).

5. Small variations in these parameters do not materially affect the determination of σ_2. Because the statistical uncertainty of our data precludes the simultaneous extraction of the α_i and σ_2 projecting from results for α in pp scattering at $\sim$250 GeV/c (V. Bartenev et al., Phys. Rev. Letts. 31, 1367 (1973)) we fix the α_i parameters at the reasonable values $\alpha_i = 0$.

6. The diffractive and electromagnetic amplitudes are of comparable magnitude in only a small range of momentum transfers, and are, in any case, likely to be approximately orthogonal in phase.

7. H. Genzel and W. Pfeil, Landolt-Börnstein 25, 157 (1975).

8. G. Fäldt, Nucl. Phys. B43, 591 (1972).

9. C. Bemporad et al., Nucl. Phys. B51, 1 (1973).

10. The differential cross-section for Coulomb production of an object of mass m, at an incident neutron momentum p_{inc}, peaks at $t = 2t_{min}$, where $t_{min} \approx (m^2-m_n^2)^2/(2p_{inc})^2$. For m near the $p\pi^-$ threshold and $p_{inc} \approx 300$ GeV/c, t_{min} corresponds to a distance on the order of 100 fm.

11. The spectrometer's angular resolution (55 μrad) was determined by fitting the resolution broadened Coulomb calculation to the measured differential cross section on Pb, at very small t, for masses near $\Delta(1236)$. We have also included in our analysis effects of multiple Coulomb scattering in the targets.

12. R. M. Edelstein, et al., Phys. Rev. Lett. 38, 185 (1977). For a recent review of other experiments and analyses, see U. Amaldi et al., An. Rev. Nuc. Sci. 26, 385 (1976).

13. See, for example, W. Beusch et al., Phys. Letts. 55B, 97 (1975).

14. G. Fäldt, Proc. of Topical Meeting on High Energy Collisions, at ICTP, Trieste (1976).

Figure Captions

1 (a) Differential cross section for neutron dissociation into $p\pi^-$ on copper, for 1.35 GeV < m < 1.45 GeV.

(b) A-dependence of the cross section for the same mass range as in (a). The solid and dashed curves are the results of model calculations discussed in the text. (Several typical error bars are shown on the data points.)

2 (a) Mass spectra for neutron dissociation into $p\pi^-$ systems on C, Al, Cu, and Pb, for $t' < .001$ $(GeV/c)^2$, and

(b) for $0.005 < t' < .03$ $(GeV/c)^2$.

In (a) the calculated contribution from Coulomb production in Pb is shown as a shaded band.

(c) Total cross sections of the produced $p\pi^-$ system on nucleons for several $p\pi^-$ mass intervals.

Table I - Coherent Production Cross-Sections for $n + A \rightarrow p\pi^- + A$

$M(p\pi^-)$ (GeV)	P_{inc} [a] (GeV/c)	Cross Section [b] (mb) for $0.0 < t' < .03$ $(GeV/c)^2$							
		Be	C	Al	Ti	Cu	Ag	Ta	Pb
1.165-1.25	100-150	.23 ± .03	.32 ± .05	.63 ± .09	1.1 ± .2	1.6 ± .2	2.9 ± .4	4.7 ± .7	5.3 ± .7
	150-200	.22 ± .03	.28 ± .04	.62 ± .09	1.0 ± .2	1.5 ± .2	2.8 ± .4	5.0 ± .7	5.7 ± .8
	200-260	.19 ± .03	.24 ± .03	.50 ± .07	.9 ± .2	1.6 ± .2	3.0 ± .4	6.1 ± .8	7.2 ± 1.0
	260-300	.17 ± .03	.24 ± .04	.56 ± .09	1.2 ± .2	1.7 ± .2	3.4 ± .5	7.9 ± 1.2	8.8 ± 1.2
1.25 -1.35	100-150	.33 ± .04	.46 ± .06	.76 ± .1	1.2 ± .2	1.4 ± .2	2.8 ± .3	3.8 ± .5	3.6 ± .5
	150-200	.27 ± .03	.38 ± .04	.69 ± .09	.9 ± .2	1.5 ± .2	2.4 ± .3	3.2 ± .4	3.6 ± .4
	200-260	.28 ± .03	.39 ± .05	.64 ± .08	.9 ± .2	1.4 ± .2	2.3 ± .3	3.7 ± .5	4.3 ± .5
	260-300	.27 ± .04	.39 ± .05	.81 ± .11	1.1 ± .2	1.6 ± .2	2.9 ± .4	4.6 ± .6	5.2 ± .7
1.35 -1.45	100-150	.30 ± .04	.40 ± .05	.78 ± .10	.8 ± .2	1.4 ± .2	2.0 ± .2	2.5 ± .4	2.6 ± .4
	150-200	.26 ± .03	.37 ± .04	.65 ± .08	.7 ± .1	1.2 ± .1	1.6 ± .2	2.3 ± .3	2.4 ± .3
	200-260	.26 ± .03	.34 ± .04	.63 ± .08	.9 ± .1	1.2 ± .1	1.9 ± .2	2.5 ± .3	3.1 ± .4
	260-300	.27 ± .03	.39 ± .05	.78 ± .10	1.1 ± .2	1.3 ± .2	2.3 ± .3	4.0 ± .6	3.9 ± .5
1.45 -1.55	100-150	.18 ± .02	.28 ± .03	.49 ± .06	.54 ± .08	.9 ± .1	1.1 ± .2	1.6 ± .3	2.0 ± .3
	150-200	.17 ± .02	.19 ± .02	.41 ± .05	.58 ± .08	.8 ± .1	1.1 ± .1	1.5 ± .2	1.7 ± .2
	200-260	.16 ± .02	.23 ± .03	.41 ± .05	.54 ± .07	.8 ± .1	1.2 ± .2	1.8 ± .2	2.1 ± .3
	260-300	.19 ± .03	.22 ± .03	.53 ± .07	.59 ± .10	.9 ± .1	1.7 ± .2	2.5 ± .4	2.5 ± .4
1.55 -1.85	100-150	.21 ± .03	.30 ± .04	.67 ± .09	.80 ± .12	1.0 ± .1	1.4 ± .2	1.9 ± .3	2.1 ± .3
	150-200	.21 ± .03	.29 ± .04	.49 ± .06	.78 ± .11	1.0 ± .1	1.3 ± .2	1.9 ± .3	1.6 ± .2
	200-260	.19 ± .02	.29 ± .03	.50 ± .06	.65 ± .09	.9 ± .1	1.4 ± .2	1.6 ± .2	2.0 ± .3
	260-300	.24 ± .03	.31 ± .04	.70 ± .10	.88 ± .14	1.0 ± .1	1.6 ± .2	2.6 ± .4	2.5 ± .4

(a) The mean values of the incident momenta for the four momentum bands in this table are 127, 176, 230, and 275 GeV/c

(b) The errors contain statistical and systematic contributions, all added in quadrature.

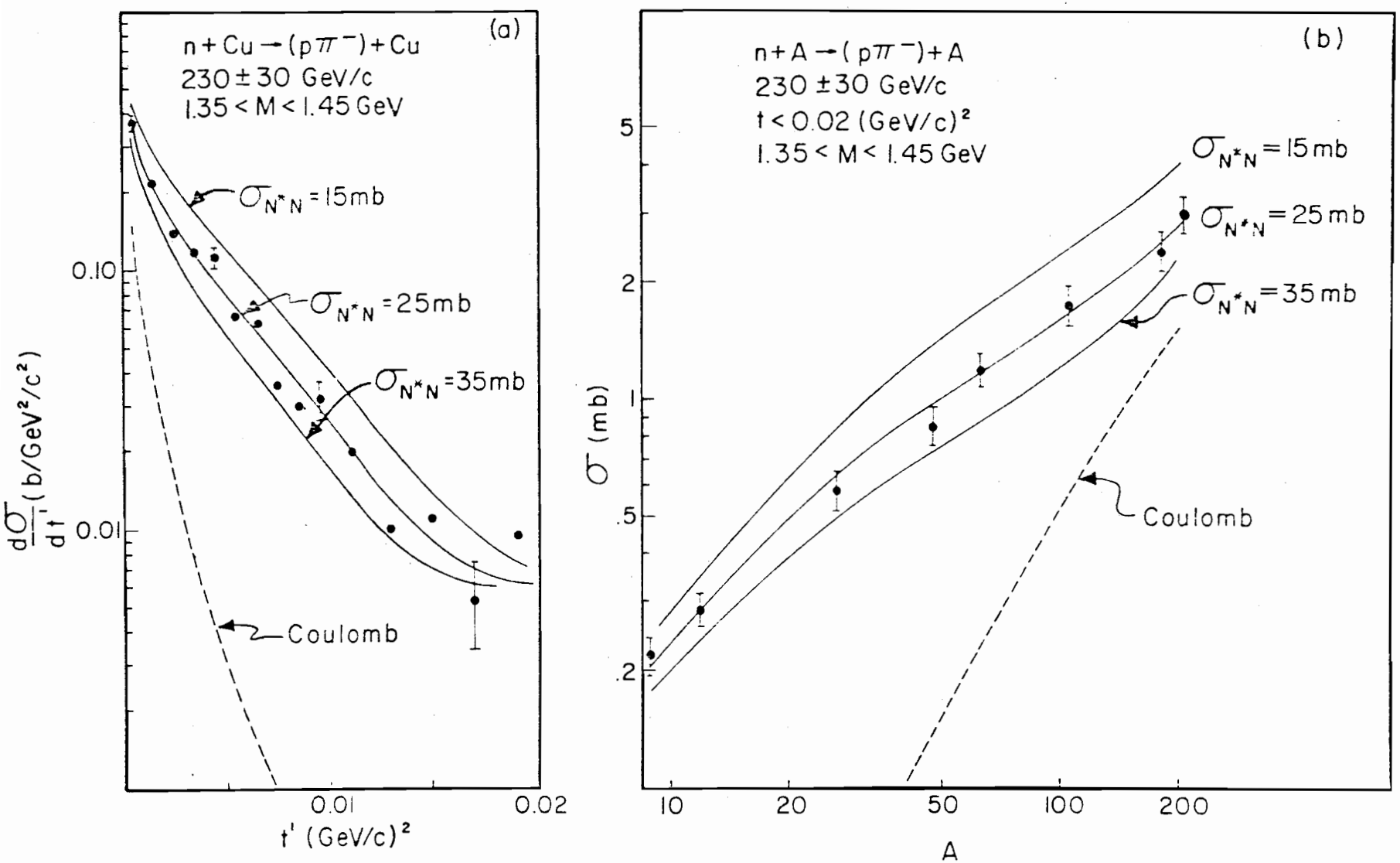
(a)
n + Cu → (pπ⁻) + Cu
230 ± 30 GeV/c
1.35 < M < 1.45 GeV
σ_N*N = 15mb
σ_N*N = 25mb
σ_N*N = 35mb
Coulomb
0.10
0.01
0.01
0.02
t' (GeV/c)²
dσ/dt' (b/GeV²/c²)
(b)
n + A → (pπ⁻) + A
230 ± 30 GeV/c
t < 0.02 (GeV/c)²
1.35 < M < 1.45 GeV
σ_N*N = 15 mb
σ_N*N = 25 mb
σ_N*N = 35 mb
Coulomb
5
2
1
.5
.2
σ (mb)
10
20
50
100
200
A

1

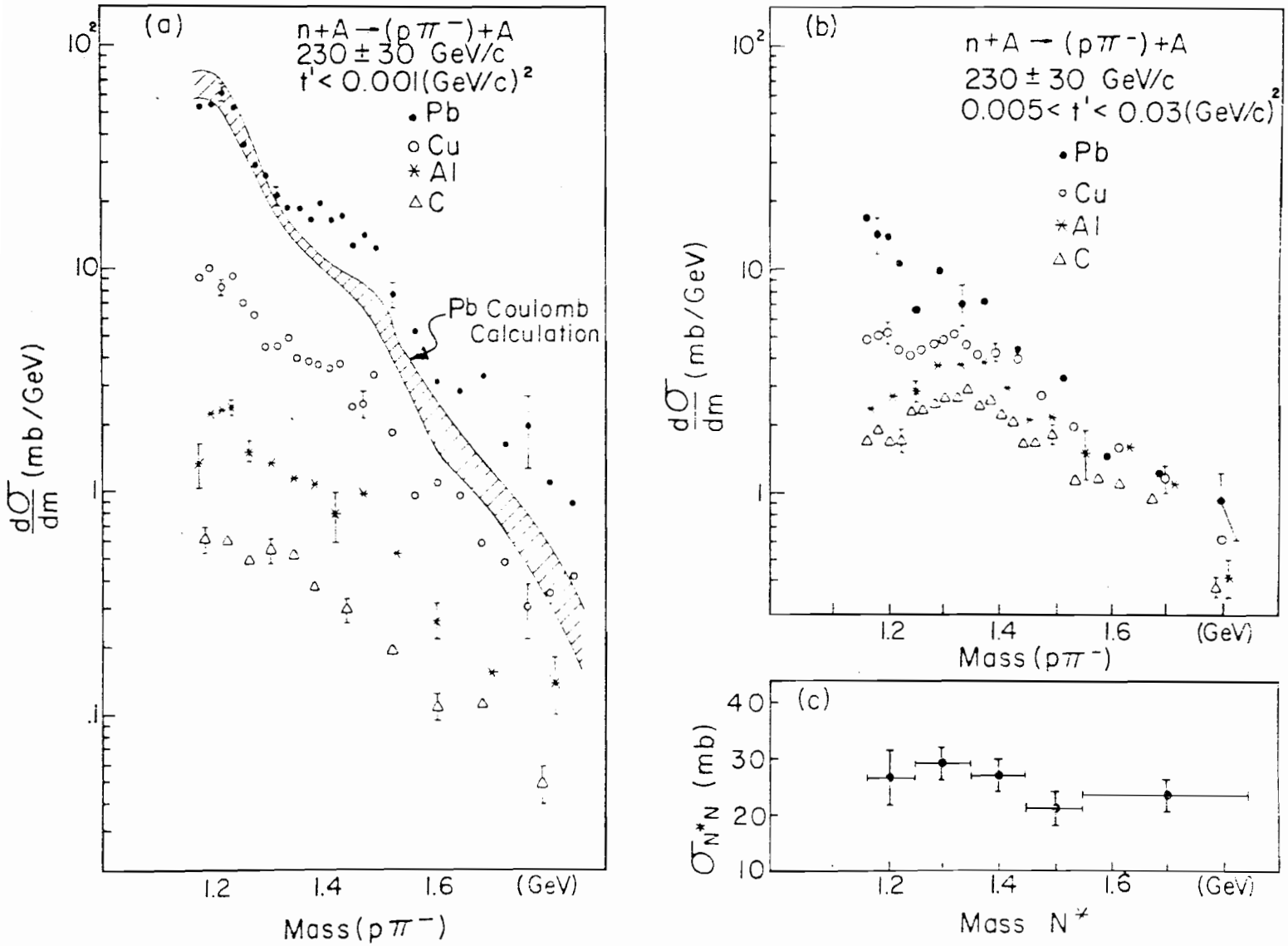
(a)
n+A → (pπ⁻)+A
230 ± 30 GeV/c
t' < 0.001(GeV/c)²
• Pb
○ Cu
* Al
△ C
Pb Coulomb Calculation
dσ/dm (mb/GeV)
Mass (pπ⁻)
(b)
n+A → (pπ⁻)+A
230 ± 30 GeV/c
0.005 < t' < 0.03(GeV/c)²
• Pb
○ Cu
* Al
△ C
dσ/dm (mb/GeV)
Mass (pπ⁻)
(c)
σ N*N (mb)
Mass N*
(GeV)

2